NUMERICAL ANALYSIS OF BUILT-UP GFRP COMPOSITE BEAMS

Libor Žáček*,1

*Libor.Zacek@vut.cz
[1]Brno University of Technology, Faculty of Civil Engineering, Veveří 331/95, 602 00 Brno, Czech Republic

Abstract

This paper deals with the issue of built-up composite beams made of GFRP (Glass Fibre Reinforced Polymers). Numerical models were analysed using the finite element method by ANSYS software. The primary focus is on evaluating the influence of bolt spacing on the ultimate load-bearing capacity and mechanical behaviour of the beams. The study aims to identify key parameters affecting the mechanical behaviour of built-up GFRP composite beams and provide insights into the influence of bolt spacing.

Keywords

GFRP, numerical analysis, built-up beam, bolted connection

1 INTRODUCTION

Composite materials have been increasingly used in the construction industry in recent decades due to their exceptional properties, particularly high mechanical strength and resistance to environmental influences. Glass Fibre Reinforced Polymers (GFRP) are included among these materials, i.e., polymer composites reinforced with glass fibres. These materials are characterized by low weight, high strength, and corrosion resistance, making them suitable for demanding applications, such as auxiliary bridge structures, facade panels, or structures exposed to aggressive environment, including marine piers or underground utility tunnels.

Composite materials are defined as a combination of two or more synergistically interacting components that differ in physical form or chemical composition [1]. Although built-up composite bars have been used in practice, their mechanical behaviour has been studied only to a limited extent. Scientific research typically focuses on elements subjected to axial forces or their shear capacity [2], [3], whereas numerical analyses often investigate bars with bonded plates [4].

In this paper describes a numerical analysis of built-up composite beams subjected to bending. The numerical analysis focuses on the load-bearing capacity of the beam and the influence of bolt spacing on its structural performance. The dependence of beam deflection at mid-span and normal stress on the lower surface of the bottom flange on the applied force was examined in the numerical model. Based on these results, the bending capacity and moment of inertia of the beam were determined. This research compared the results of numerical simulations of beams with varying bolt spacing to those of a beam without bolt holes, to quantify their effect on the overall load-bearing capacity of the structure.

2 METHODOLOGY

Three built-up beams with different bolt-hole spacing were compared in this paper. The beams are composed of two U-profiles (180×60/8) made of GFRP, connected by bolts with a diameter of 12 mm. The axial distances of the holes in the longitudinal direction were set to 600 mm, 300 mm, and 150 mm. Two rows of bolts were considered in all cases in the vertical direction, illustrated in Fig 1. and Fig 2. The beams were modelled as simply supported, with their supports provided by steel cylinders with a diameter of 50 mm. The load was applied at the midspan of the beam by vertical displacement of the loading cylinder simulating the effect of press. In the numerical model, a cylinder with a rounded end of 100 mm radius was used to represent the press, as required by the standard for testing GFRP materials [5].

Received 07/02/2025/Accepted 12/05/2024/ Published 30/09/2025 DOI 10.13164/juniorstav.2025.25037

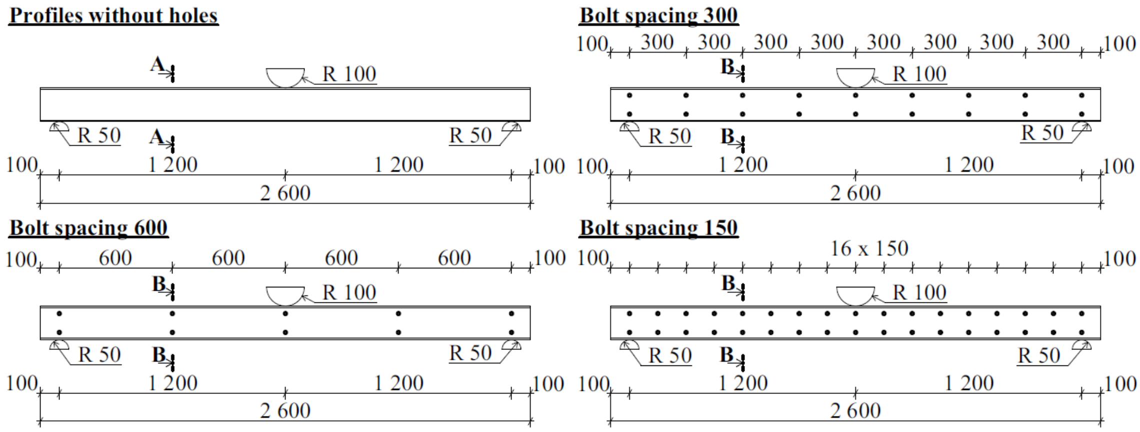

Fig. 1 Analysed beams with different bolt spacing.

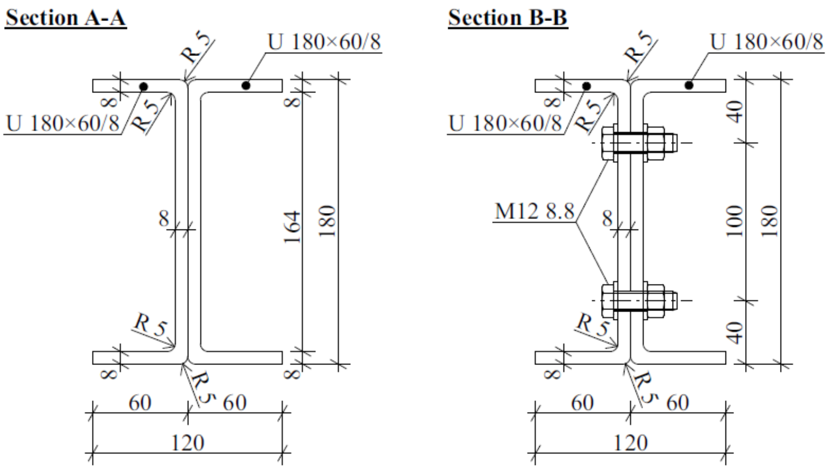

Fig. 2 Analysed beams with a different cross-section of the beam.

The analysis was carried out in ANSYS 2019 R2 [6], a system based on the finite element method. The material model for GFRP was defined as a linear isotropic material with Young's modulus of 35 GPa and a Poisson's ratio of 0.2. The material model for steel was defined as a bilinear isotropic (elastic-plastic) material, with an elastic modulus of 210 GPa and a Poisson's ratio of 0.3. The plastic behaviour was characterized by yield stress, which depended on the specific material used, followed by a small strain hardening. The yield strength corresponded to the material used for the supports and the loading cylinder.

The model also included contact interactions between the profiles, loading cylinder and supports. The contacts were defined as frictional, with a friction coefficient of 0.2.

Boundary conditions were set to restrict both horizontal and transverse displacements. Boundary conditions preventing displacement in the horizontal, transverse, and longitudinal directions were applied to the edges of the supports. The boundary condition restricting displacement in the transverse directions was applied to the edges of the bolt holes to simulate the influence of mechanical connection by the bolts, which were not included in the numerical model. Fig 3. shows the meshing of the model.

DOI 10.13164/juniorstav.2025.25037

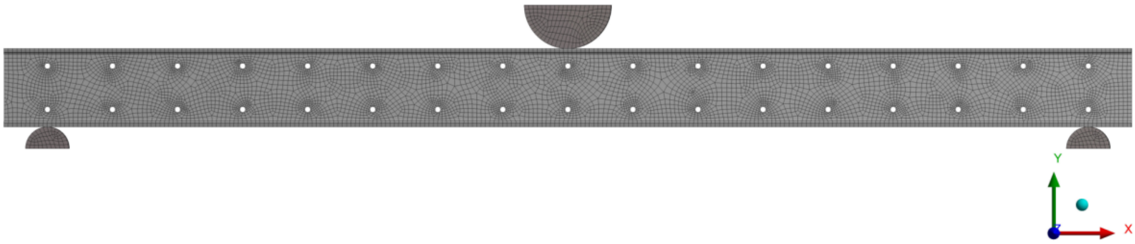

Fig. 3 Meshed model of the beam with a 150 mm bolt spacing.

The element sizes of individual components are listed in Tab 1. The number of nodes and finite elements is provided in Tab 2. The holes in the profile were modelled with a clearance of 1 mm, meaning that for a bolt M12, the hole diameter was 13 mm.

Tab. 1 Size of finite elements.

	U-Profiles	**Supports**	**Load cylinder**
Size [m]	0.015	0.010	0.010

Tab. 2 Number of nodes and finite elements.

	Number of nodes	**Number of finite elements**
Profiles without holes	102,713	20,598
Bolt spacing 600 mm	138,034	25,096
Bolt spacing 300 mm	159,006	28,784
Bolt spacing 150 mm	197,554	35,544

The goal of the numerical analysis was to monitor the vertical deflection and normal stress at the midspan of the beam in dependence on the force applied at midspan. The force was introduced into the model through vertical displacement applied to the upper surface of the press head. The displacement magnitude was set to 35 mm and was used in 100 loading steps.

The bending capacity was determined from the results of the numerical analysis based on the characteristic bending strength and compared with the bending capacity of profiles without hole-induced weakening. The bending capacity of profiles without holes was calculated using equation (1)

First, the bending moment at the midpoint of the beam, M_E, was calculated using equation (2).

The stress at the lower flange was extracted from the numerical model results for the corresponding moment. The bending moment at which the normal stress in the extreme fibres reaches the material's characteristic bending strength was determined using direct proportionality. This moment is referred to as the effective bending capacity $M_{R,eff}$. The influence of the holes on the bending capacity is quantified by the ratio of $M_{R,eff}$ to M_R.

$$M_R = \frac{I_y \cdot f_{m,k}}{z} \tag{1}$$

Where $f_{m,k}$ represents the ultimate bending stress parallel to fibres, taken from tables as 240 MPa, the moment of inertia I_y in mm^4 and z is the distance from the neutral axis to the extreme fibres which was calculated based on the cross-section dimensions in mm.

$$M_E = \frac{F \cdot L}{4} \tag{2}$$

Where F is the force applied at the midpoint of the beam in N, L is the span length in mm. The force loading the beam was obtained as the sum of the reactions at both supports.

DOI 10.13164/juniorstav.2025.25037

The effective moment of inertia can be derived from the beam deflection based on the modification of the deflection equation by rearranging equation (3), and the effective moment of inertia can be expressed by equation (4), The influence of the holes on the moment of inertia and thus bending stiffness was quantified by the ratio of $I_{y,eff}$ to I_y.

$$u_z = \frac{1}{48} \cdot \frac{F \cdot L^3}{E \cdot I_y} \tag{3}$$

$$I_{y,eff} = \frac{1}{48} \cdot \frac{F \cdot L^3}{E \cdot u_z} \tag{4}$$

F is the force applied at the midpoint of the beam in N, L is the span length in mm, E is the Young's modulus of the material in bending in MPa and u_z represents the beam deflection at mid-span in mm.

3 RESULTS

The cross-section characteristics for the built-up beam without hole-induced weakening are presented in Tab 3. The values required for determining the effective moments of inertia and the effective bending capacity were extracted from the numerical models and are listed in Tab 4. Fig 4. shows the beam's vertical deflection and Fig 5. shows normal stress distribution. The determination of effective moments of inertia and effective bending capacity for different bolt spacing as well as the evaluation of the influence of holes on load-bearing capacity, is provided in Tab 5.

Tab. 3 Characteristics of the gross cross-section.

	Moment of inertia I_y [mm^4]	**Bending moment capacity M_R [Nmm]**
Channel section 180×60/8	20,062,672	53.50×10^6

Tab. 4 Results of the numerical analysis.

	Load F [N]	**Normal stress σ_x [MPa]**	**Vertical deformation u_z [mm]**
Profiles without holes	84,342	221.30	34.59
Bolt spacing 600 mm	84,366	223.25	34.60
Bolt spacing 300 mm	84,374	223.26	34.64
Bolt spacing 150 mm	82,918	222.02	34.66

Tab. 5 Evaluation of results.

	Effective bending moment capacity $M_{Rd,eff}$ [Nmm]	**Effective moment of inertia $I_{y,eff}$ [mm^4]**	**$\frac{I_{y,eff}}{I_y}$ [mm^4]**	**$\frac{M_{R,eff}}{M_R}$ [Nmm]**
Profiles without holes	53.51×10^6	20,064,011	1.000	1.000
Bolt spacing 600 mm	53.50×10^6	20,063,921	1.000	0.992
Bolt spacing 300 mm	53.44×10^6	20,042,653	0.999	0.992
Bolt spacing 150 mm	52.49×10^6	19,685,421	0.981	0.980

DOI 10.13164/juniorstav.2025.25037

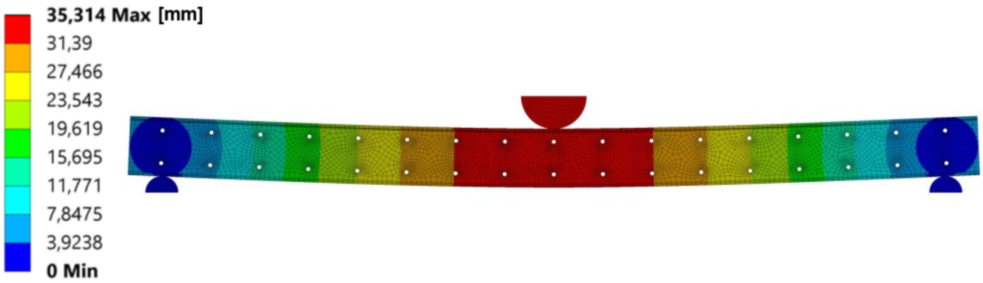

Fig. 4 Visualization of the beam vertical deflection u_z [mm].

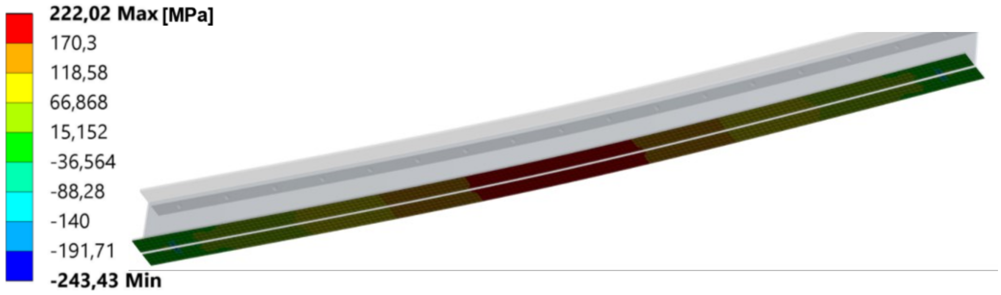

Fig. 5 Normal stress distribution on the bottom face of the bottom flange σ_x [MPa].

4 DISCUSSION

The influence of bolt-holes spacing on the load-bearing capacity of built-up GFRP beams was examined in this study. The results indicate that as the hole spacing changed, changes occur in the effective bending capacity $M_{Rd,eff}$ and the effective moment of inertia $I_{y,eff}$. The bending capacity M_{Rd} and the moment of inertia I_y of a composite built-up beam without openings, composed of two U-profiles (180×60/8) were determined as a reference value.

It was observed from the results of the numerical simulations, that a decrease in hole spacing leads to a gradual reduction in both the effective bending capacity and the effective moment of inertia. While the differences between the reference and effective values are minimal for the largest spacing, a noticeable reduction in parameters was recorded for the smallest spacing (150 mm), indicating an influence of the holes on the overall mechanical behaviour of the beam.

The ratios between the reference and effective values of the bending capacity and the moment of inertia confirmed this trend. These ratios are very close to 1 for hole spacings of 600 mm and 300 mm, suggesting minimal reduction in mechanical properties. Reducing the bolt spacing to 150 mm leads to increased differences between these parameters with the effective moment of inertia reaching, in the worst case, 98% of the reference value. The bending capacity at a hole spacing of 150 mm decreased to approximately 98% of its original value.

A similar trend was observed in support reactions, normal stress, and deformations. Although the differences between the individual variants were relatively small, a systematic decrease in load-bearing capacity with decreasing hole spacing was identified.

DOI 10.13164/juniorstav.2025.25037

5 CONCLUSION

The numerical analysis showed that bolt-hole spacing influences the load-bearing capacity and stiffness of built-up beams. While the changes in mechanical parameters are negligible for larger spacings (600 mm, 300 mm), a slight reduction in effective bending capacity and moment of inertia was observed at a spacing of 150 mm.

The results suggest that, in the practical design of structures using built-up profiles, the influence of hole spacing on mechanical properties does not need to be significantly considered unless extremely small spacings are used. In such cases, local reinforcement of the profiles or other measures to improve bending capacity may be appropriate.

This study provides a basis for further research focused on the experimental verification of the numerical results.

Acknowledgements

This work was supported by the research programme of the Faculty of Civil Engineering, Brno University of Technology No FAST-S-24-8586.

References

[1] ALTIN KARATAŞ, Meltem and Hasan GÖKKAYA. 2018. A review on machinability of carbon fiber reinforced polymer (CFRP) and glass fiber reinforced polymer (GFRP) composite materials. Defence Technology [online]. 14(4), 318-326 [accessed 2024-12-2]. DOI: 10.1016/j.dt.2018.02.001. ISSN 22149147. Available at: https://linkinghub.elsevier.com/retrieve/pii/S2214914717302040

[2] BOSCATO, Giosue', Carlo CASALEGNO and Salvatore RUSSO. 2015. Performance of built-up columns made by pultruded FRP material. Composite Structures [online]. 121, 46-63 [accessed 2024-4-18]. DOI: 10.1016/j.compstruct.2014.11.022. ISSN 02638223. Available at: https://linkinghub.elsevier.com/retrieve/pii/S0263822314005911

[3] ZHANG, Qifeng, Zuohong XU and Yuqing HU. 2023. Built-Up Fiber-Reinforced Polymers (FRP) Profiles with Improved Shear Performance for FRP–Concrete Hybrid Section. Buildings [online]. 13(9) [accessed 2024-4-25]. DOI: 10.3390/buildings13092298. ISSN 2075-5309. Available at: https://www.mdpi.com/2075-5309/13/9/2298

[4] MINGHINI, Fabio, Nerio TULLINI, Francesco ASCIONE and Luciano FEO. 2019. Numerical failure analysis of built-up columns composed of closely spaced pultruded FRP channels. Composite Structures [online]. 207, 478-487 [accessed 2024-4-25]. DOI: 10.1016/j.compstruct.2018.09.016. ISSN 02638223. Available at: https://linkinghub.elsevier.com/retrieve/pii/S0263822318326163

[5] EN 13706-2 Reinforced plastics composites - Specifications for pultruded profiles - Part 2: Methods of test and general requirements. European Committee for Standardization, 2007.

[6] ANSYS® Academic Research Release 2019 R2.

DOI 10.13164/juniorstav.2025.25037